Kinetic Studies on Enzyme-Catalyzed Reactions: Oxidation of Glucose, Decomposition of Hydrogen Peroxide and Their Combination

Zhimin Tao,[‡] Ryan A. Raffel,[‡] Abdul-Kader Souid,[†] and Jerry Goodisman[‡*]
[†]Department of Pediatrics, State University of New York, Upstate Medical University, Syracuse, New York 13210; and [‡]Department of Chemistry, Syracuse University, Syracuse, New York 13244

ABSTRACT The kinetics of the glucose oxidase-catalyzed reaction of glucose with O_2, which produces gluconic acid and hydrogen peroxide, and the catalase-assisted breakdown of hydrogen peroxide to generate oxygen, have been measured via the rate of O_2 depletion or production. The O_2 concentrations in air-saturated phosphate-buffered salt solutions were monitored by measuring the decay of phosphorescence from a Pd phosphor in solution; the decay rate was obtained by fitting the tail of the phosphorescence intensity profile to an exponential. For glucose oxidation in the presence of glucose oxidase, the rate constant determined for the rate-limiting step was $k = (3.0 \pm 0.7) \times 10^4\ M^{-1}s^{-1}$ at 37°C. For catalase-catalyzed H_2O_2 breakdown, the reaction order in $[H_2O_2]$ was somewhat greater than unity at 37°C and well above unity at 25°C, suggesting different temperature dependences of the rate constants for various steps in the reaction. The two reactions were combined in a single experiment: addition of glucose oxidase to glucose-rich cell-free media caused a rapid drop in $[O_2]$, and subsequent addition of catalase caused $[O_2]$ to rise and then decrease to zero. The best fit of $[O_2]$ to a kinetic model is obtained with the rate constants for glucose oxidation and peroxide decomposition equal to 0.116 s^{-1} and 0.090 s^{-1} respectively. Cellular respiration in the presence of glucose was found to be three times as rapid as that in glucose-deprived cells. Added NaCN inhibited O_2 consumption completely, confirming that oxidation occurred in the cellular mitochondrial respiratory chain.

INTRODUCTION

We study two enzyme-catalyzed reactions, the oxidation of glucose and the breakdown of hydrogen peroxide, by monitoring oxygen concentration using phosphorescence decay. Previous studies of these reactions did not monitor oxygen concentration; the measurements presented in this study permit confirmation of the values of some rate constants, and show problems in the previously assumed model. We study the combination of the two reactions, and also the combination of the reactions with cellular respiration. The latter gives information about the efficiency of glucose transport into cells in vitro.

Measurement of $[O_2]$ based on quenching of the phosphorescence of Pd (II)-meso-tetra-(4-sulfonatophenyl)-tetrabenzoporphyrin was first introduced by Vanderkooi et al. (1), Rumsey et al. (2), and Pawlowski and Wilson (3). This method, which allows accurate and sensitive determination of $[O_2]$ in biological systems (4), uses the time constant τ for the decay of the phosphorescence of the Pd phosphor in solutions; $1/\tau$ is a linear function of $[O_2]$ (see Eq. 8). We have used the method previously to monitor cellular respiration (mitochondrial O_2 consumption) under various conditions (5–8). This method was also used by us to study rapid chemical oxidation in solutions, in particular the dithionite reaction (9).

We study the glucose oxidase-catalyzed oxidation of glucose, the catalase-accelerated breakdown of hydrogen peroxide, their combination in cell-free culture, and glucose-driven cellular respiration. Previous studies of glucose oxidase and catalase did not involve monitoring changes in $[O_2]$; by doing this, we can get additional information about the mechanism of the reactions. In addition, values of the rate constants are obtained that, in some cases, differ significantly from those previously published. Given their critical roles in fundamental biochemical and biophysical studies, the kinetic properties of these enzymes deserve more attention from researchers.

Although glucose oxidase is not very specific, its action on glucose is faster than on other sugars (10). The reaction of glucose ($C_6H_{12}O_6$) with O_2 produces glucono-δ-lactone ($C_6H_{10}O_6$) and H_2O_2, as follows.

$$\text{glucose} + O_2 \rightarrow \text{glucono-}\delta\text{-lactone} + H_2O_2.$$

In aqueous solutions, glucono-δ-lactone ($C_6H_{10}O_6$) reacts spontaneously with water to form gluconic acid ($C_6H_{12}O_7$), so the overall reaction is

$$C_6H_{12}O_6 + H_2O + O_2 \rightarrow C_6H_{12}O_7 + H_2O_2. \quad (1)$$

Glucose oxidase has a unique specificity for β-D-glucose with no action on its α-anomer (10,11). However, in solutions, α-D-glucose mutarotates to β-D-glucose (12,13). Thus, the reaction of β-D-glucose is accompanied by the mutarotation

$$\alpha\text{-D-glucose} \underset{k_\beta}{\overset{k_\alpha}{\rightleftharpoons}} \beta\text{-D-glucose}.$$

This conversion is catalyzed by acid as well as specific substances (14). A free intermediate with the open-chain

Submitted July 3, 2008, and accepted for publication November 20, 2008.

*Correspondence: goodisma@mailbox.syr.edu

Abdul-Kader Souid's present address is Department of Paediatrics, Faculty of Medicine and Health Sciences, United Arab Emirates University, PO Box 17666, Al Ain, United Arab Emirates.

Editor: Patrick Loria.

0006-3495/09/04/2977/12 $2.00

doi: 10.1016/j.bpj.2008.11.071

aldehyde form equilibrates with both α- and β-D-glucose, but its concentration is negligible (~26 ppm) (14). The interconversion of the isomers is slow, so we assume an equilibrium mixture, with only the β-D-glucose available for reaction. (Glucose oxidase preparations are sometimes contaminated by *mutarotase* (13), which accelerates mutarotation of α-D-glucose to β-D-glucose.) The $\alpha \rightarrow \beta$ conversion constant k_α is higher than that for $\beta \rightarrow \alpha$, k_β (14). Le Barc'H et al. (15) have reported k_α and k_β at various temperatures and concentrations. Interpolating their values, we find $k_\alpha = 1.60 \pm 0.09\ h^{-1}$ and $k_\beta = 1.09 \pm 0.07\ h^{-1}$ at 37°C, so that the mutarotation equilibrium constant $K \equiv k_\alpha/k_\beta$ is equal to 1.46 ± 0.13, and the equilibrium distribution is 59.3% β-isomer. Initially, one has

$$[\beta\text{-D-glucose}]_{eq} = \frac{K}{1+K}[\text{D-glucose}]_0,$$

where $[\text{D-glucose}]_0$ is the sum of the two anomer concentrations.

In the presence of glucose oxidase, Eq. 1 involves the sequence of reactions (10)

$$E_{ox} + \beta\text{-D-glucose} \xrightarrow{k_1} E_{red}P_1 \xrightarrow{k_2} E_{red} + P_1 \qquad (2)$$

$$E_{red} + O_2 \xrightarrow{k_3} E_{ox}P_2 \xrightarrow{k_4} E_{ox} + P_2. \qquad (3)$$

The enzyme oxidizes β-D-glucose to glucono-δ-lactone (P_1), and O_2 re-oxidizes the enzyme, producing H_2O_2 (P_2).

The generated H_2O_2 (P_2) can further decompose into H_2O + 1/2 O_2 through a thermodynamically favorable process. This process becomes much faster with certain catalysts present, including the transition metal compounds (for instance, Fe^{3+} and Mn^{4+}) and many peroxidases that contain such ions in their enzymatic structures. As the most common and efficient enzyme, catalase, with its four porphyrin heme subunits, breaks down H_2O_2 at a very high turnover rate. Although the exact mechanism of catalase-accelerated H_2O_2 decomposition remains unclear, a proposed reaction strategy through the transient existence of a catalase-H_2O_2 intermediate has been established (16,17).

$$\text{Fe(III)-catalase} + H_2O_2 \xrightarrow{k_i} O = \text{Fe(IV)-catalase} + H_2O \qquad (4)$$

$$H_2O_2 + O = \text{Fe(IV)-catalase} \xrightarrow{k_{ii}} \text{Fe(III)} - \text{catalase} + H_2O + O_2 \qquad (5)$$

Fe (III) in the enzyme heme group serves as the electron source, thus rendering one electron to H_2O_2 molecule and forming an intermediate, compound I (16). Then the distorted heme ring reacts with a second H_2O_2 molecule to restore the original ferricatalase. In these two steps, H_2O_2 acts first as an oxidizing, then a reducing agent. Because there exist few reports illustrating the kinetic aspects of the reaction steps or testing the assumptions of the kinetic model, the following studies are of interest.

MATERIALS AND METHODS

Reagents

The Pd (II) complex of meso-tetra-(4-sulfonatophenyl)-tetrabenzoporphyrin (sodium salt, Pd phosphor) was obtained from Porphyrin Products (Logan, UT); its solution (2.5 mg/mL = 2 mM) was prepared in dH_2O and stored at −20°C in small aliquots. D (+) glucose anhydrous (Lot No. D00003205) was purchased from Calbiochem (La Jolla, CA). Glucose oxidase (from *Aspergillus niger;* 1,400 units/mL in 100 mM sodium acetate, pH ~4.0) was purchased from Sigma-Aldrich (St. Louis, MO). Catalase (from bovine liver; 2950 units/mg solid or 4540 units/mg protein) and hydrogen peroxide (30 wt % solutions in water, i.e., ~10.6 M; Lot No. 04624AH) were both purchased from Sigma (the quality and concentration of H_2O_2 were guaranteed for 2 years). Catalase was made in 10 mg/mL solution immediately before experiments and never frozen for reuse. Working solutions of H_2O_2 (106 mM) were freshly made in dH_2O right before injection. NaCN solution (1.0 M) was freshly prepared in dH_2O and the pH was adjusted to ~7.0 with 12 N HCl immediately before use. Phosphate buffered salt solution (PBS, without Mg^{2+} and Ca^{2+}) and RPMI-1640 cell culture media were purchased from Mediatech (Herndon, VA). T-cell lymphoma (Jurkat) cells were cultured as described (5–8).

The rate equation of glucose oxidase-catalyzed glucose oxidation

If the equilibrium between α- and β-D-glucose is established rapidly, Eqs. 2 and 3 are rate controlling. The reaction rate is $R = d[P_1]/dt = d[P_2]/dt = -d[O_2]/dt$. At steady state, the rates of all steps are equal, so

$$R = k_1[E_{ox}][\beta\text{-D-glucose}] = k_2[E_{red}P_1] = k_3[E_{red}][O_2] = k_4[E_{ox}P_2].$$

Letting C be the total enzyme concentration (here ~0.125 μM), i.e., $C = [E_{ox}] + [E_{red}P_1] + [E_{red}] + [E_{ox}P_2]$, we have

$$C = \frac{k_4[E_{ox}P_2]}{k_1[\beta\text{-D-glucose}]} + \frac{k_4[E_{ox}P_2]}{k_2} + \frac{k_4[E_{ox}P_2]}{k_3[O_2]} + [E_{ox}P_2].$$

The rate is $R = k_4[E_{ox}P_2]$ and the specific rate is $v = R/C = -C^{-1}\, d[O_2]/dt$, so

$$\frac{1}{v} = \frac{\frac{k_4}{k_1[\beta\text{-D-glucose}]} + \frac{k_4}{k_2} + \frac{k_4}{k_3[O_2]} + 1}{k_4} = \frac{1}{k_1[\beta\text{-D-glucose}]} + \frac{1}{k_2} + \frac{1}{k_3[O_2]} + \frac{1}{k_4}, \qquad (6)$$

showing $1/v$ is a linear function of both $[\beta\text{-D-glucose}]^{-1}$ and $[O_2]^{-1}$. The above equations are also valid if the α–β equilibration is slow enough to neglect; in this case only the initial (equilibrium) concentration of [β-D-glucose] is relevant.

The rate equation of catalase-catalyzed decomposition of hydrogen peroxide

Rewriting reactions 4 and 5 with E representing Fe (III)-catalase and I the intermediate, compound I, we have:

$$E + H_2O_2 \xrightarrow{k_i} I + H_2O$$

$$H_2O_2 + I \xrightarrow{k_{ii}} E + H_2O + O_2.$$

Let E_0 be the total enzyme (here ~0.40 μM), i.e., $[E_0] = [E] + [I]$. The reaction rate (R) is $R = d[O_2]/dt$. At steady state, the rates of the two steps are equal, so $k_i\ [E][H_2O_2] = k_{ii}[I][H_2O_2]$. This leads to $[E_0] = \frac{k_i + k_{ii}}{k_i}[E]$, or $[E] = \frac{k_{ii}}{k_i + k_{ii}}[E_0]$, and the rate becomes

$$R = k_{ii}[I][H_2O_2] = k_i[E][H_2O_2] = \frac{k_i k_{ii}}{k_i + k_{ii}}[E_0][H_2O_2], \tag{7}$$

and the specific rate, $v = R/[E_0] = [E_0]^{-1}d[O_2]/dt$, is

$$v = \frac{1}{[E_0]} \times \frac{d[O_2]}{dt} = \frac{k_i k_{ii}}{(k_i + k_{ii})}[H_2O_2] = k_{hp}[H_2O_2].$$

Instrumentation

The home-made O_2 analyzer was described previously (5,6). In our instrument, the solution containing the phosphor is flashed 10 times per second by a visible (670 nm) light source (flash duration, 100 μs). The intensity of the phosphorescence is recorded every 3.2 μs, and the decreasing part of the intensity profile (after the light source is turned off) is fit to an exponential $Ae^{-t/\tau}$ to find the decay constant τ. DAZYlab (Measurement Computing Corporation, Norton, MA) was used for data acquisition. The data were analyzed by a Microsoft Visual C^{2+} language program (9) that calculated the phosphorescence lifetime (τ) and decay constant ($1/\tau$). A typical phosphorescence profile is shown in Fig. 1. Like most of the measurements described in this study, it was made at 37°C. The sample, in PBS, contained 2 μM Pd-phosphor, 0.5% bovine fat-free albumin, 7 units/mL glucose oxidase, and 800 μM glucose, in sealed vials. For this profile only, intensity was measured every 2 μs. The flash goes on at $t = t_0$ ~22.87 ms, stays on with a constant intensity until $t = t_1$ ~22.97 ms, and then goes off, so flash duration is 100 μs. To determine τ, we localized the time of the peak intensity and fitted the decreasing part of the profile to an exponential (9). The fit, shown as a solid gray line in Fig. 1, gave the decay rate $1/\tau = 3.2\ ms^{-1}$ or $\tau = 311\ \mu s$. Because O_2 quenches the phosphorescence, the decay rate $1/\tau$ is a linear function of $[O_2]$:

$$1/\tau = 1/\tau_0 + k_q[O_2], \tag{8}$$

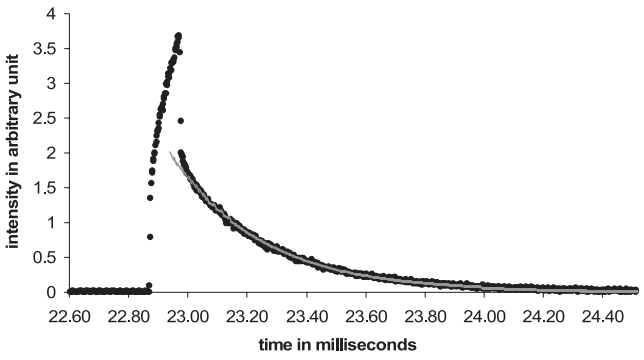

FIGURE 1 A typical phosphorescence profile. The sample, in PBS, contained 2 μM Pd-Phosphor, 0.5% bovine fat-free albumin, 7 units/mL glucose oxidase and 800 μM glucose. Sampling was at 500,000 Hz. The flash goes on at $t = t_0$ ~22.87 ms, stays on with a constant intensity until $t = t_1$ ~22.97 ms, and then goes off, so flash duration is 100 μs. The decay part of the profile was fit to an exponential $A\ e^{-t/\tau}$ (*gray line*) to calculate the lifetime τ. The fit gave $\tau = 311\ \mu s$ (decay rate $1/\tau = 3.2\ ms^{-1}$).

where $1/\tau_0$ is the decay rate in the absence of O_2 and k_q the quenching constant. The data were composed of a number of profiles like that of Fig. 1. The C^{2+} program screened the data stream for intensities >0.05. In every 0.1 s interval, it located the time of each maximum (t_1), and found the best-fit exponential from data after the maximum. It thus generated 10 decay constants per second, which were averaged.

Calibration with glucose oxidase

A Clark-type O_2 electrode was used to determine $[O_2]$ in PBS solution containing glucose oxidase (7.0 units/mL), 50–250 μM D-glucose, 2 μM Pd phosphor, and 0.5% fat-free bovine serum albumin. The plot of $[O_2]$ versus [D-glucose] (Fig. 2 *A*) was linear (r^2 >0.999), with slope = 1.05 μM O_2 per μM glucose, demonstrating a stoichiometry of 1:1, as in Eq. 1.

We then used our instrument to measure $1/\tau$ for solutions containing D-glucose at concentrations between 0 and 1000 μM. For each concentration, $1/\tau$ was determined as the average of 1000–2000 measurements.

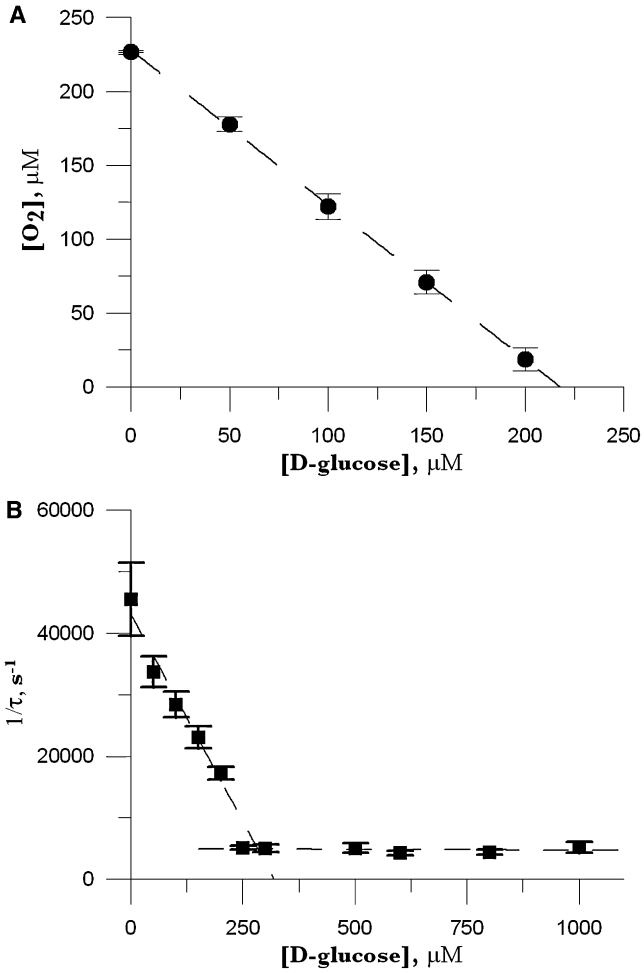

FIGURE 2 (*A*) Calibration with glucose oxidase. The solution (at 37°C) in PBS contained 7.0 units/mL glucose oxidase, 0.05–1.0 mM D-glucose, 2 μM Pd phosphor, and 0.5% fat-free bovine serum albumin. A Clark-type O_2 electrode was used to measure dissolved O_2. Apparent stoichiometry (moles O_2 consumed per mole glucose added) was 1.05 (r^2 >0.999). (*B*) Establishing stoichiometry from decay rate. Phosphorescence decay was measured in glucose solutions in air-saturated water ($[O_2]$ ~237 μM) containing glucose oxidase. Values of $1/\tau$ were plotted versus [glucose] and fitted to two lines, the second, horizontal, is for $[O_2] = 0$; the intersection shows [glucose]/O_2 = 1:1.

Results are shown in Fig. 2 *B* (error bars show the standard deviations, which are worse for smaller values of τ). The best fit to a two-line function (Fig. 2 *B*, *dashed lines*) was

$$\begin{cases} 1/\tau = \alpha_1 + \beta_1[\text{D-glucose}], 0 < [\text{D-glucose}] \leq 283\ \mu\text{M} \\ 1/\tau = \alpha_2, 283 < [\text{D-glucose}] \leq 1000\ \mu\text{M} \end{cases}$$

with $\alpha_1 = 43{,}844\ \text{s}^{-1}$, $\beta_1 = -146.7\ \mu\text{M}^{-1}\text{s}^{-1}$, and $\alpha_2 = 4788\ \text{s}^{-1}$, whereas the intersection is ([D-glucose], $1/\tau$) = (266.2 μM, 4788 s^{-1}). Because $[O_2]$ is 267 μM for air-saturated water at 25°C, this confirms the stoichiometry: [D-glucose]/$[O_2]$ = 1:1. It also determines the value of the quenching rate constant, k_q = 134.5 ± 14.3 $\mu\text{M}^{-1}\ \text{s}^{-1}$, and the value of $1/\tau_0$, 5002 ± 437 s^{-1}.

Stability of hydrogen peroxide

The stability of hydrogen peroxide was checked by high performance liquid chromatography (HPLC). The analysis was carried out on a Beckman reversed-phase HPLC system, which consisted of an automated injector (model 507e) and a pump (model 125). The column, 4.6 × 250 mm Beckman Ultrasphere IP column, was operated at room temperature (25°C) at a flow rate of 0.5 mL/min. The run time was 30 min and the mobile phase was dH_2O. Ten microliters 30 wt % H_2O_2 was diluted in 2 mL dH_2O and 5–50 μL injections were run on HPLC, which corresponded to 260–2600 pmol H_2O_2. The detection wavelength was fixed at 250 nm. A typical HPLC chromatogram is shown in Fig. 3 *A*.

A single peak was always observed at retention time ~5 min in all the samples. The area of this peak was evaluated. Measurements were carried out in two different days spanning the time period over which the H_2O_2 experiments were carried out. The variations of H_2O_2 peak areas for the same injection were found to be between 1.8% and 6.7%. Thus, it is clear that the hydrogen peroxide used in this study is stable. In addition, H_2O_2 peak areas (*A*, arbitrary units) were proportional to the injected amount of H_2O_2. The best linear fit to the results, shown in Fig. 3 *B*, was $A \times 10^{-6} = (0.00337 \pm 0.00012)\ (H_2O_2) + (0.551 \pm 0.184)$ where (H_2O_2) is in pmol and $r^2 = 0.976$.

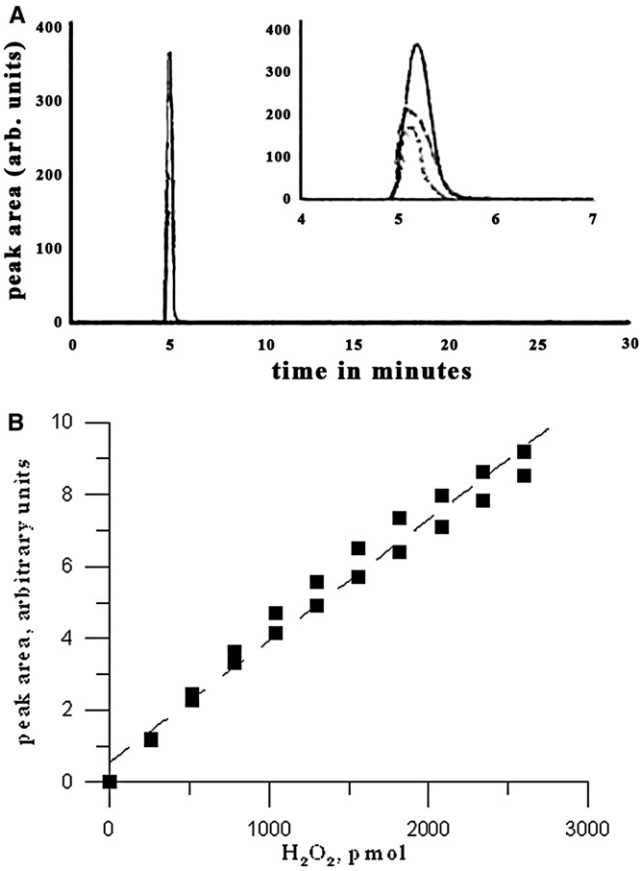

FIGURE 3 Stability of H_2O_2 in solutions checked by HPLC. Samples were run at room temperature (25°C) at a flow rate of 0.5 mL/min. The detection wavelength was 250 nm, the run time was 30 min and the mobile phase was dH_2O. Ten μL of 30 wt. % H_2O_2 was diluted in 2 mL dH_2O; 5–50 μL injections, which corresponded to 260-2600 pmol H_2O_2, were then run on HPLC. (*A*) Representative HPLC chromatograms of H_2O_2. The three plots, from bottom to top, are due to independent injections of 530 (*dotted line*), 1060 (*dashed line*), and 2120 (*solid line*) pmol H_2O_2. A single peak was observed at retention time ~300 seconds in three samples; the inset panel shows the peak region. (*B*) H_2O_2 peak areas (*A*, arbitrary units) assumed proportional to the injected amount of H_2O_2, are fitted to a linear function $A \times 10^{-6} = 0.00337\ [H_2O_2] + 0.551$ ($r^2 = 0.976$). For each concentration, measurements were taken in two different days covering H_2O_2 usage period. The variations of H_2O_2 peak areas for the same injection were 1.8%–6.7%.

RESULTS

Kinetics of glucose oxidase-catalyzed glucose oxidation

We first studied the glucose oxidase reaction at 37°C in the presence of D-glucose. If Eqs. 2 and 3 are rate-controlling, the specific rate is given by Eq. 6. This shows $1/\nu$ is a linear function of both $[\beta\text{-D-glucose}]^{-1}$ and $[O_2]^{-1}$. If the α–β equilibration is not rapid, the α-to-β conversion reactions must be taken into account. However, if the α-to-β equilibration is extremely slow, it may be neglected, provided that the initial concentration of β-D-glucose only is considered. We do this in the following.

In our experiments, D-glucose was first dissolved in PBS (pH ~7.4) at 37°C, and then injected into PBS containing glucose oxidase. Measured $[O_2]$ as a function of t is shown in Fig. 4 *A* for 50 μM ≤ [D-glucose] ≤ 300 μM; the reaction rate is the negative slope of the curve. Each experiment was repeated 3–5 times; the representative plots are shown in Fig. 4 *A*. Each data set is fit to an exponential $\text{Pe}^{-\text{Qt}}$ (Fig. 4 *A*, *lines*). The initial rate $v_o = -d[O_2]/dt$ is then *PQ*. For the lowest glucose concentration, the reaction rate is essentially zero for $t > 200$ s, so the neglect of the mutarotation is not justified. Thus, for experiments at 50 μM glucose, v_o is calculated from an exponential fit to only the first half of the data (fit not shown in Fig. 4 *A*). Calculated v_o are shown in Fig. 4 *B*.

The initial specific rate should obey (Eq. 6)

$$\frac{1}{v_0} = \frac{A}{[\text{D-glucose}]_0} + B, \tag{9}$$

where

$$A = \frac{1+K}{k_1 K} \quad \text{and} \quad B = \frac{1}{k_2} + \frac{1}{k_3[O_2]} + \frac{1}{k_4}.$$

A plot of $1/v_0$ versus $1/[\text{D-glucose}]_0$ with 50 ≤ [D-glucose]$_0$ ≤ 300 μM is shown in Fig. 4 *B*. It should be noted

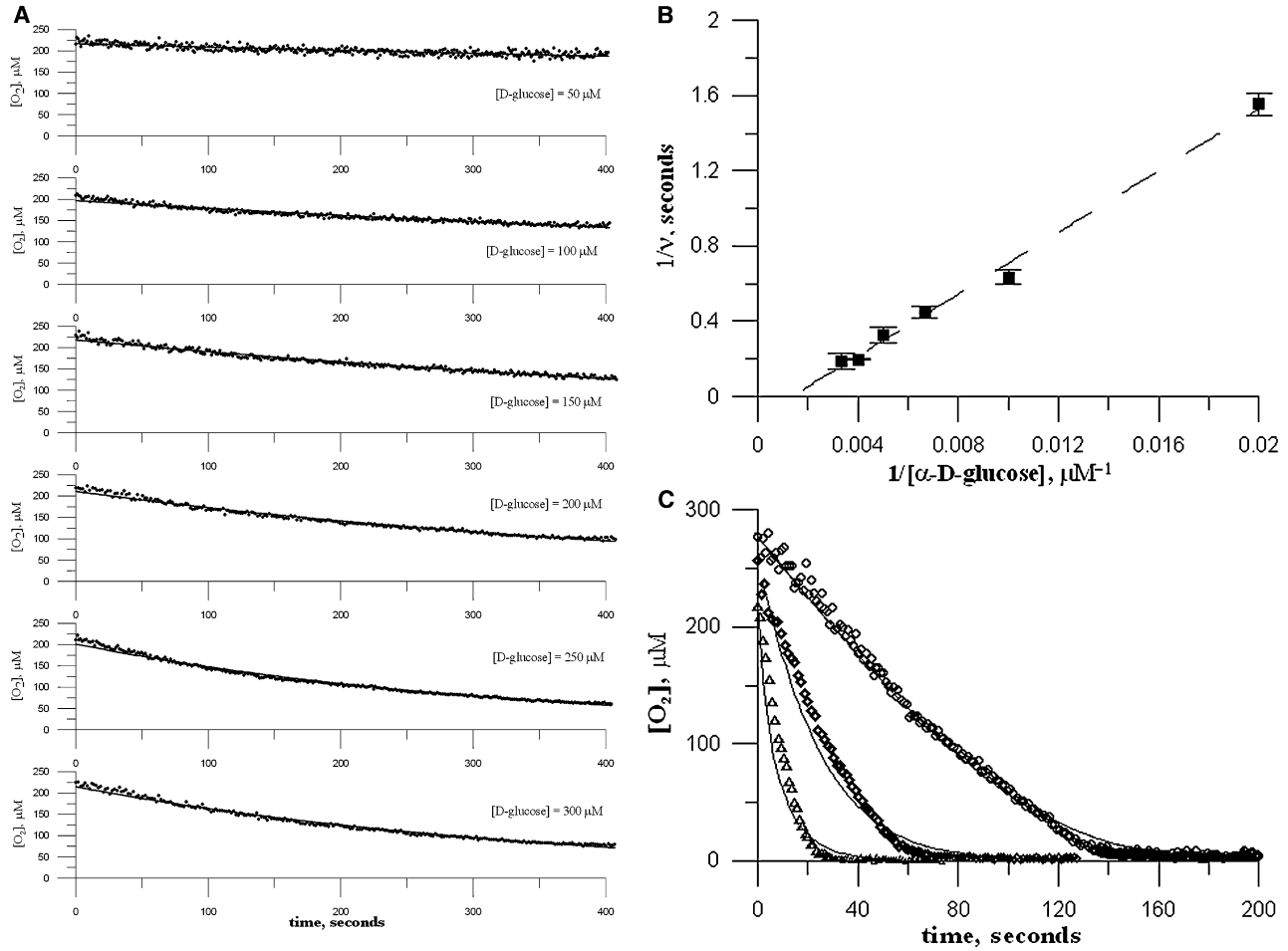

FIGURE 4 Kinetics of glucose oxidase.(*A*) D-glucose was injected into PBS containing glucose oxidase (pH ~7.4; 50 μM $\leq$ [D-glucose] $\leq$ 300 μM) at 37°C. $[O_2]$ as a function of t (*solid dots*) was fit to an exponential function (*gray solid line*). (*B*) Plot of $1/v_0$ (v_0 = initial rate) versus $1/[\text{D-glucose}]_0$ (*solid squares*). Error bars are the standard deviation from two to three experiments for each concentration. The data were fit to a line with slope = 55.4 $\pm$ 3.5 μM s and intercept = 0.032 $\pm$ 0.003 s ($r^2 > 0.984$). From the slope one gets the mutarotation equilibrium constant for glucose. (*C*) O_2 consumption in the presence of glucose oxidase. Glucose in excess over O_2 is added at time zero. From left to right, [D-glucose] = 10 mM (*triangles*), 5 mM (*diamonds*), 1 mM (*circles*), respectively. The results are fit to Eq. 10 (*solid lines*).

that the small error bars on the points do not include the errors inherent in the conversion of τ to $[O_2]$. The best linear fit gives $A = 55.4 \pm 3.5$ μM s and $B = 0.032 \pm 0.003$ s ($r^2 > 0.984$). The value of B is essentially zero, implying k_2, k_3, and k_4 are very large. Using the determined value of A with $K = 1.46$ (15), we find the value of the rate constant $k_1 = 0.030$ μM^{-1} s^{-1} at 37°C, comparable to the reported 0.016 $\mu M^{-1} s^{-1}$ (10).

Fig. 4 *C* shows the O_2 consumption in the presence of glucose oxidase when glucose is present in excess over O_2 (from left to right, [D-glucose] = 10, 5, and 1 mM, respectively). With [glucose] >> $[O_2]$, the exact integral of Eq. 6 from t_0 to t is

$$\alpha\left([O_2] - [O_2]_0\right) + b\left(\ln[O_2] - \ln[O_2]_0\right) = -(t - t_0). \tag{10}$$

Here, $[O_2]_0$ corresponds to $[O_2]$ in air-saturated PBS,

$$\alpha = \frac{1}{C}\left(\frac{1}{k_1[\text{glucose}]} + \frac{k_2 + k_4}{k_2 k_4}\right),$$

and $b = (Ck_3)^{-1}$. Using the Excel Solver function, we fit the curves of Fig. 4 *C* to Eq. 10, obtaining $\{a, b\}$ in $\{\mu M^{-1}$ s, s$\}$ = (−0.034, 11.7), (0.025, 20.4), and (0.295, 22.1) from left to right respectively. (Uncertainty about the zero of time may be the reason the fits are not perfect: note that all the fits could be improved by shifting the times for the experimental points slightly to the left.) The value of a increases as [glucose] decreases, whereas the value of b is relatively constant.

From a linear plot of a versus 1/[glucose], we obtain $1/k_1 = 44.4 \pm 3.0$ μM s, so that $k_1 = (2.3 \pm 0.2) \times 10^4$ M^{-1} s^{-1}, and $(k_2 + k_4)/k_2k_4 = -0.00734 \pm 0.00178$ s. (The experiments shown in Fig. 4, *A* and *B*, gave $k_1 = 3.0 \times 10^4$ M^{-1} s^{-1}.) The very small value of $(k_2 + k_4)/k_2k_4$ implies large numerical

values for k_2 and k_4. Using the average value of b, 18.1 ± 5.6 s, and enzyme concentration $C = 0.125$ μM, k_3 is calculated as $(4.4 \pm 1.4) \times 10^5$ M^{-1} s^{-1}. These results may be compared to those reported by Gibson et al. (10), $k_1 = 1.6 \times 10^4$ M^{-1} s^{-1} and $k_3 = 2.4 \times 10^6$ M^{-1} s^{-1} at 38°C.

The initial rate of reaction, obtained by differentiating Eq. 10, is

$$\left(\frac{d[O_2]}{dt}\right)_0 = -V_0 = -\left(a + \frac{b}{[O_2]_0}\right)^{-1}. \quad (11)$$

Using $[O_2]_0 = 225$ μM in Eq. 11, we find, for [glucose] = 10, 5, and 1 mM, $V_0 = 55.1$, 8.7, and 2.5 μM s^{-1}, respectively.

Kinetics of catalase-aided decomposition of hydrogen peroxide

As indicated in Eqs. 4 and 5, catalase reacts with one mole of H_2O_2 to produce the intermediate I, which then reacts with another mole of H_2O_2 to regenerate the enzyme and release one mole of O_2. The reaction rate $R = d[O_2]/dt$ is given by

$$R = k_{ii}[I][H_2O_2] = k_i[E][H_2O_2] = \frac{k_i k_{ii}}{k_i + k_{ii}}[E_0][H_2O_2].$$

Thus, the specific rate $v = R/[E_0] = [E_0]^{-1}d[O_2]/dt$, leading to

$$v = \frac{1}{[E_0]} \times \frac{d[O_2]}{dt} = \frac{k_i k_{ii}}{(k_i + k_{ii})}[H_2O_2] = k_{hp}[H_2O_2], \quad (12)$$

with $k_{hp} = (\frac{k_i k_{ii}}{k_i + k_{ii}})$. According to Eq. 12, v is proportional to $[H_2O_2]$ and the catalase-catalyzed decomposition of H_2O_2 is a first-order reaction with respect to H_2O_2.

To confirm the order of the reaction, we carried out the following experiments. At 37°C, air-saturated PBS solutions containing 2 μM Pd phosphor and 0.1 mg/mL catalase were placed in sealed containers for oxygen measurement. A value of $1/\tau$ was acquired every 0.1 s. Various H_2O_2 concentrations were added at ~1 min and measurement was continued until >3 min. The measured values of $1/\tau$, which depends linearly on $[O_2]$, are plotted versus t in Fig. 5 *A*. Each plot corresponds to an experiment in which H_2O_2 at the indicated concentration was added to air-saturated PBS. The rapid climb in $[O_2]$ when H_2O_2 is injected is evident. Because the reaction rate is independent of $[O_2]$, the plots show an essentially linear increase in $1/\tau$ from $t = t_l$ (l for low O_2 level) to $t = t_h$ (h for high O_2 level). To establish the order with respect to H_2O_2 and to calculate rate constant k_{hp}, we compare measured rates of reaction for different $[H_2O_2]$. The analysis used in this study is similar to that in previous studies of dithionite kinetics (9).

For each plot, the values of $1/\tau$ before and after the rise in $[O_2]$, $1/\tau_l$ and $1/\tau_h$, were obtained by averaging 600 measurements at early ($0 \le t \le t_l$) and late ($t_h \le t \le 180$ s) times, respectively. The value of $1/\tau_l$ should correspond to $[O_2]$ in air-saturated PBS, which is 267 μM at 37°C, whereas the value of $1/\tau_h$ corresponds to total $[O_2]$ after H_2O_2 decomposition, i.e., the sum of original $[O_2]$ and $[O_2]$ produced by the catalase-catalyzed decomposition of H_2O_2. Therefore, the difference between the values of $1/\tau_l$ and $1/\tau_h$ reflects the produced O_2. The white lines in Fig. 5 *A* are best fits of the experimental data to the two-parameter function,

$$\begin{aligned} 1/\tau &= 1/\tau_l \; t < t_l \\ &= 1/\tau_1 + (t - t_l)(1/\tau_h - 1/\tau_l)/(t_h - t_l) t_l \le t \le t_h \\ &= 1/\tau_h \; \tau > t_h. \end{aligned} \quad (13)$$

Given $1/\tau_l$ and $1/\tau_h$, we find the values of the two variable parameters t_l and t_h by minimizing the sum of the square deviations of Eq. 13 from experimentally measured $1/\tau$. The rate $R = d[O_2]/dt$ is obtained by dividing $d(1/\tau)/dt$ by k_q (see Eq. 8), the derivative being calculated from the linearly-increasing portion of the plots, i.e.,

$$\begin{aligned} R = \frac{d[O_2]}{dt} &= \frac{1}{k_q}\left(\frac{1}{\tau_h} - \frac{1}{\tau_l}\right)(t_h - t_l)^{-1} \\ &= \left(k_{hp} \times [E_0]\right)[H_2O_2]^x. \end{aligned} \quad (14)$$

The value of k_q here is expected to be different from that obtained from the glucose study, because different enzymatic systems are detected here; the new value of k_q can be determined from a regression of $(1/\tau_h - 1/\tau_l)$ versus generated $[O_2]$ (because the stoichiometry is known to be generated $[O_2] = 1/2\,[H_2O_2]$), and gives 93.0 ± 9.1 $\mu M^{-1}s^{-1}$. The same experiments were also carried out at 25°C in PBS solutions, and analyzed in the same way; results are shown in Fig. 5 *B*.

In Eq. 14 we write the rate as $k_{hp}[E_o]$ times $[H_2O_2]^x$ where x is the order of the reaction with respect to H_2O_2. To find x, we carry out linear regression of $\ln(R)$ versus $\ln([H_2O_2])$ (Fig. 5 *C*). At 37°C the slope is 1.27 ± 0.14, so that the overall reaction is approximately first order in H_2O_2. This result, x ~1, agrees with the report by Beers and Sizer (18), who measured the order by monitoring rapid change in H_2O_2 absorptions during the reaction. The rate of the reaction (in $\mu M\ s^{-1}$) is found to be equal to

$$\begin{aligned} R &= \frac{d[O_2]}{dt} \\ &= \exp(-3.656 + 1.266 \ln[H_2O_2]) \approx 0.177[H_2O_2]. \end{aligned} \quad (15)$$

In contrast, the slope of the linear fit of $\ln(R)$ versus $\ln([H_2O_2])$ is 1.69 ± 0.14 for 25°C, suggesting that the reaction becomes 1-1/2-order at the lower temperature. In particular,

$$\begin{aligned} R = \frac{d[O_2]}{dt} &= \exp(-6.615 + 1.692 \ln[H_2O_2]) \\ &\approx 4.49 \times 10^{-3}[H_2O_2]^{1.5} \end{aligned}$$

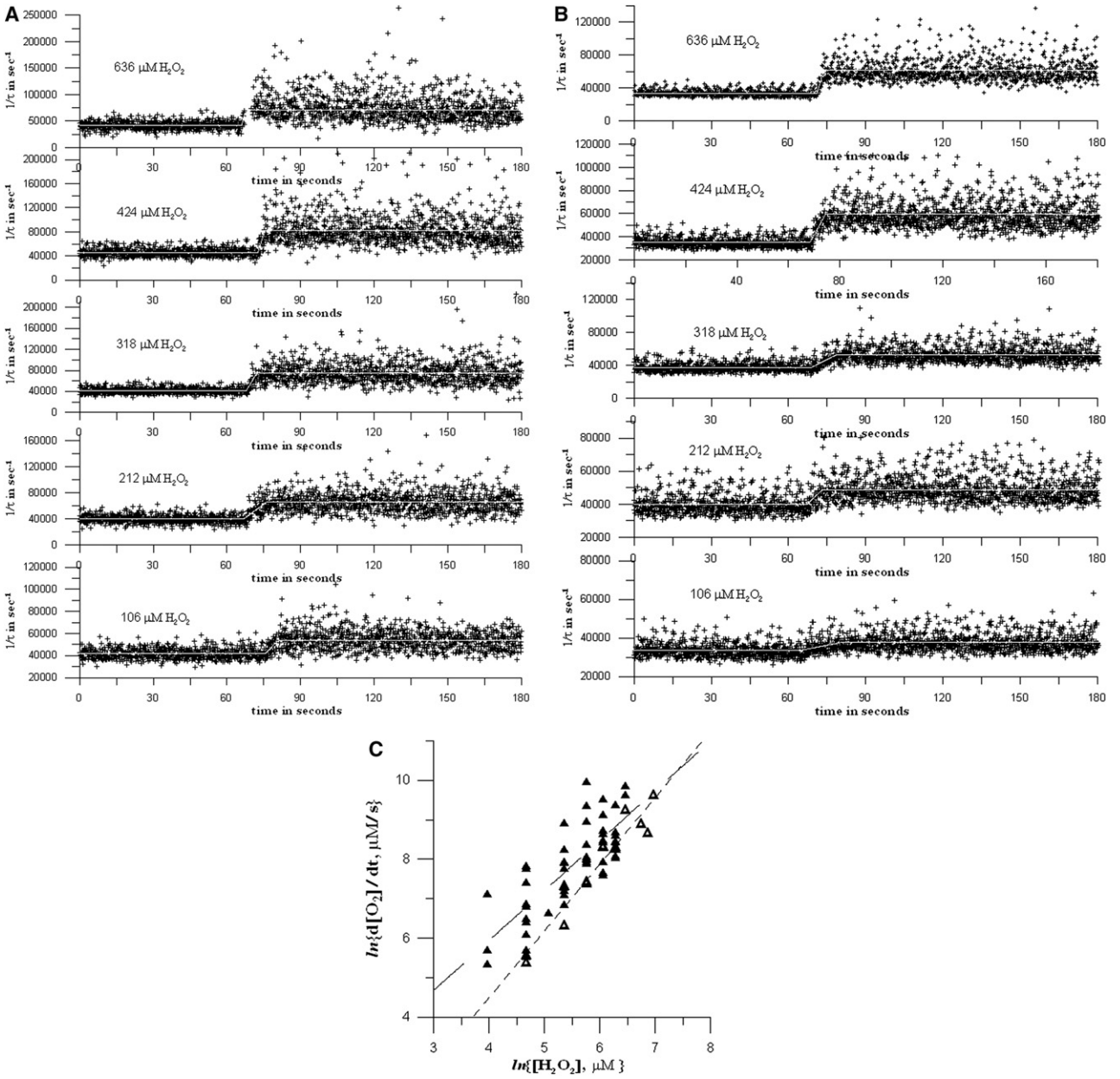

FIGURE 5 Decomposition of H_2O_2 in the presence of 0.1 mg/mL catalase at (*A*) 37°C and at (*B*) 25°C. The reaction (in PBS) contained 2.0 μM Pd phosphor, 0.5% albumin, and 106–636 μM H_2O_2 as labeled. The rapid increase in $1/\tau$ when H_2O_2 is injected corresponds to its catalyzed breakdown to generate O_2. The white solid lines indicate the best fits of experimental data (*solid dots*) to a three-line function. Slope of middle line gives reaction rate. (*C*) Logarithms of reaction rates are plotted against logarithms of $[H_2O_2]$ at 25°C (*open triangles*) and 37°C (*solid triangles*). Linear fits to the two sets of data are shown. Open triangles fit by the dotted line show the results at 25°C, whereas solid triangles fit by the dashed line represent the results at 37°C.

at 25°C (all concentrations in units of μM). Not only does the rate constant depend on temperature, but, apparently, so does the reaction order. Other researchers reported the reaction rate in the catalase-catalyzed breakdown of H_2O_2 was only slightly altered with changing temperature (600 cal activation energy) (18). However, those results were acquired from reactions at low ionic strength whereas ours were obtained in phosphate buffer with a high ionic strength. More importantly, we suggest that the importance of the elementary reactions not included in Eqs. 4 and 5 may change with temperature.

Thus, we propose a more general reaction mechanism by including the reverse of Eq. 4, so that the mechanism becomes

$$E + H_2O_2 \underset{k_{-i}}{\overset{k_i}{\leftrightarrow}} I + H_2O \tag{16}$$

$$H_2O_2 + I \overset{k_{ii}}{\rightarrow} E + H_2O + O_2.$$

At steady state,

$$\frac{d[I]}{dt} = k_i[E][H_2O_2] - k_{-i}[I] - k_{ii}[I][H_2O_2] = 0,$$

which gives

$$[I] = \frac{k_i[E][H_2O_2]}{k_{-i} + k_{ii}[H_2O_2]},$$

and the reaction rate is

$$R = \frac{d[O_2]}{dt} = k_{ii}[I][H_2O_2] = \frac{k_i k_{ii}[E][H_2O_2]^2}{k_{-i} + k_{ii}[H_2O_2]}.$$

Since $[E_0] = [E]+[I]$,

$$[E_0] = [E] + \frac{k_i[E][H_2O_2]}{k_{-i} + k_{ii}[H_2O_2]} = \left\{\frac{k_{-i} + (k_i + k_{ii})[H_2O_2]}{k_{-i} + k_{ii}[H_2O_2]}\right\}[E]$$

which gives

$$R = \frac{d[O_2]}{dt} = \frac{k_i k_{ii}[H_2O_2]^2}{k_{-i} + k_{ii}[H_2O_2]} \times \frac{k_{-i} + k_{ii}[H_2O_2]}{k_{-i} + (k_i + k_{ii})[H_2O_2]}[E_0] = \frac{k_i k_{ii}[E_0][H_2O_2]^2}{k_{-i} + (k_i + k_{ii})[H_2O_2]}. \quad (17)$$

If k_{-i} is negligible, Eq. 17 becomes

$$R = \frac{d[O_2]}{dt} = \frac{k_i k_{ii}[E_0]}{(k_i + k_{ii})}[H_2O_2],$$

which is 1st order with respect to H_2O_2. However, if the value of k_{-i} is large in comparison with $(k_i + k_{ii})[H_2O_2]$, the reaction rate approaches $\frac{k_i k_{ii}}{k_{-i}}[E_0][H_2O_2]^2$, which is 2nd order in $[H_2O_2]$. Thus, if k_{-i} is not negligible, the reaction order in terms of H_2O_2 should appear to be between 1 and 2. Because the rate constants k_i, k_{-I}, and k_{ii} depend on temperature differently, the apparent order of reaction may change with temperature as well. In particular, our results suggest that, when temperature decreases, k_{-i} becomes more important relative to the other rate constants, raising the reaction order.

By fitting experimental results to Eq. (17, we obtained the best values for all the kinetic constants at 37°C: $k_i = 5.0 \times 10^5$ $M^{-1}s^{-1}$, $k_{-i} = 377$ s^{-1}, and $k_{ii} = 5.6 \times 10^6$ $M^{-1}s^{-1}$. Because k_{ii} $[H_2O_2] > k_{-i}$ except for the lowest value of $[H_2O_2]$ used, the reverse reaction of Eq. 16 is negligible, making the overall reaction appear 1st order. However, the sum of the squared deviations between measured and calculated rates using Eq. 17, which has three parameters, is 5.5×10^5, only slightly below the sum of the squared deviations with the two-parameter function of Eq. 15, 5.9×10^5, so that the exact values of the rate constants cannot be taken very seriously. At 25°C, there are many fewer points and more scatter than at 37°C, so the three-parameter fit is not meaningful (many sets of values for the three parameters give the same difference between measured and calculated rates). However, the fact that the apparent order of the reaction is much greater than one suggests that k_{-i} exceeds $k_{ii}[H_2O_2]$ at the lower temperature. Because both rate constants must be lower at 25°C than at 37°C, this implies that k_{-i} has a lower activation energy than k_{ii}.

The action of glucose oxidase on glucose followed by the addition of catalase

We next studied the O_2-consuming and O_2-producing reactions together at 37°C. We injected first glucose oxidase (at ~55 s) and later catalase (at ~175 s) into RPMI-1640 media containing 10 mM D-glucose, obtaining the results in Fig. 6 *A*. The first evident drop in $[O_2]$ accompanied injection of glucose oxidase. The best fit to Eq. 10 shows $a = -0.159$ μM^{-1} s and $b = 28.3$ s; the latter differs substantially from the corresponding value in PBS, but is quite in line with the values of b for higher [glucose]. The catalase, injected after O_2 depletion by the glucose oxidation, catalyzed the decomposition of the previously produced H_2O_2, generating O_2, whose concentration climbed to ~86 μM. Then $[O_2]$ declined again to zero because of the reaction with glucose, present in excess.

According to Eq. 1, all of the original O_2 (250 ± 12 μM) should be converted into H_2O_2 in the first reaction and, according to Eqs. 5 and 6, half of the original O_2 should be re-formed by the second reaction; however, the peak concentration was only one-third of the original $[O_2]$. The decay rate of the second peak was apparently much smaller than that of the first peak, 0.0376 s^{-1} vs. 0.0846 s^{-1} (values from exponential fits). Both facts are explained by the competition between O_2 production (from H_2O_2) and consumption (catalyzed by glucose oxidase).

A first check on this involves fitting the points from 184 s to 256 s to an exponential and extrapolating back to 174 s (time at which $[O_2]$ starts to increase); this gives 118 μM, nearly half of the original $[O_2]$. For a more detailed verification, we write $d[O_2]/dt$ as the result of an O_2-producing reaction with rate constant k_p and an O_2-consuming reaction with rate constant k_c:

$$\frac{d[O_2]}{dt} = k_p[H_2O_2] - k_c[O_2] = k_p[H_2O_2]_0 e^{-k_p(t-t_p)} - k_c[O_2], \quad (18)$$

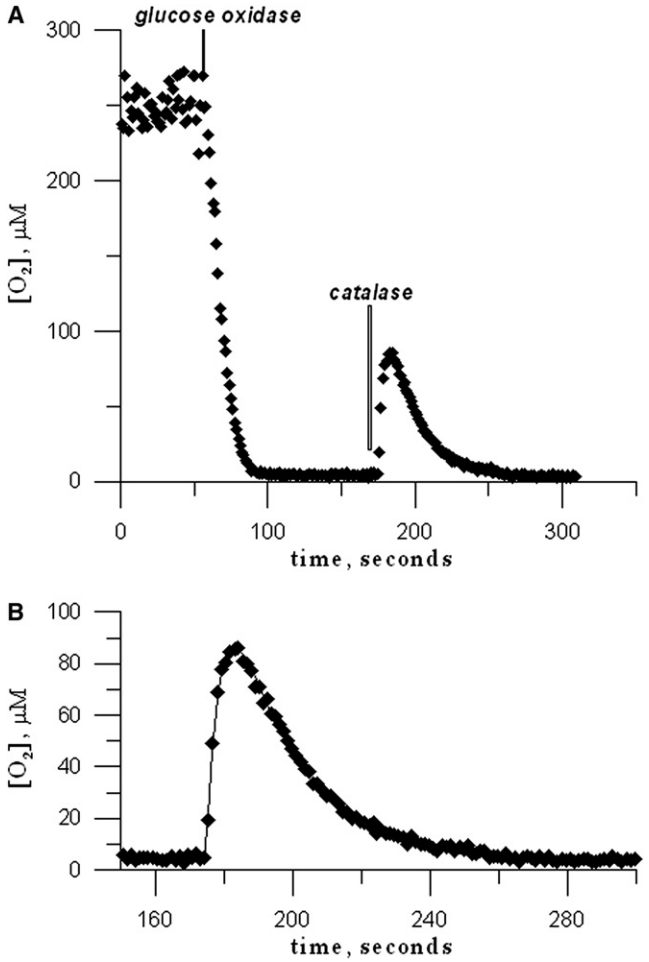

FIGURE 6 (*A*) Seven units/mL glucose oxidase was injected at $t \sim 50$ s into 1.0 mL of RPMI-1640 medium containing 10 mM glucose, causing oxygen consumption. At $t \sim 170$ s, 50 μg/mL catalase was injected, causing decomposition of H_2O_2 formed in the first reaction. (*B*) The data for $150\ \text{s} < t < 300\ \text{s}$ are well fitted by assuming that the original $[O_2]$ was converted into H_2O_2, which decomposes with rate constant k_p to re-form O_2, which is destroyed by reaction with leftover glucose with rate constant k_c. Squares = experimental results, line = fit to Eq. 18 with $k_c = 0.116\ \text{s}^{-1}$, $k_p = 0.090\ \text{s}^{-1}$.

where t_p is the time at which O_2 production begins (~174 s) and $[H_2O_2]_0$ is assumed to be equal to the original $[O_2]$ (see Eq. 1), i.e., 250 μM. The solution to Eq. 17 for $t \geq t_p$ is

$$[O_2] = \frac{k_p[O_2O_2]_0}{k_c - k_p}\left[e^{-k_p(t-t_p)} - e^{-k_c(t-t_p)}\right]. \qquad (19)$$

In (Fig. 6 *B* we show that Eq. 19, with $k_c = 0.116\ \text{s}^{-1}$ and $k_p = 0.090\ \text{s}^{-1}$, gives a good fit to the measured $[O_2]$. This k_p is comparable to the value of $0.177\ \text{s}^{-1}$ in Eq. 15. The difference apparently reflects the difference between PBS and RPMI media; the latter contains more inorganic salts, and the ionic strength is much higher. Using $k_p = 0.177\ \text{s}^{-1}$ in Eq. 18 and choosing k_c to give the best fit, k_c becomes $0.122\ \text{s}^{-1}$, which is not changed significantly from the two-parameter fitting; however, the fit becomes significantly worse.

Glucose-driven cellular respiration

The last experiments show the action of catalase in the environment of cellular respiration, which involves glucose oxidation. Jurkat cells were washed twice in PBS and incubated in PBS for 16 h to deplete glucose. Cell viability was >90% at this point. The cells (10^6 per run) were then suspended in PBS, 2 μM Pd phosphor, and 0.5% bovine serum albumin (final volume, 1.0 mL). Temperature was maintained at 37°C throughout. At time zero, 5 μL of glucose or dH_2O was added (final concentration of glucose = 100 μM). $[O_2]$ was measured every 2.0 min, alternately for the two conditions. Results are shown in Fig. 7 (*solid circles*, with glucose; *open circles*, no glucose).

In the first 38 min, the rate of oxygen consumption (k) for both conditions was 0.14 μM O_2/min, which was similar to the drift rate (0.18 μM O_2/min). After this time (that probably represents the time necessary for glucose or other substrate to enter the cell), k increased for both conditions. From 40 to 140 min, the value of k with no glucose present was 0.32 μM O_2/min ($[O_2]$ dropped from 128 μM to 96 μM); NaCN was added at 140 min. From 38 to 114 min, k with glucose present was 0.79 μM O_2/min ($[O_2]$ dropped from

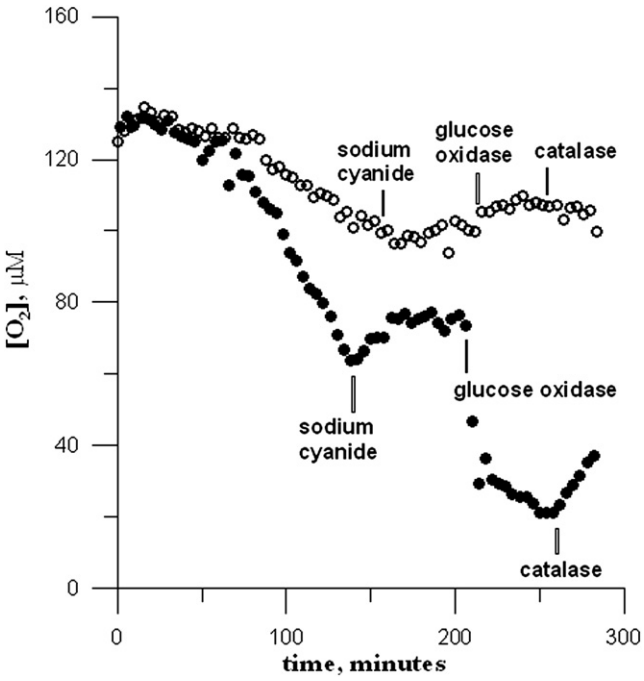

FIGURE 7 Glucose-driven respiration. Jurkat cells were washed twice in PBS and incubated in PBS for 16 h. The cells (10^6 per run) were then suspended in PBS, 2 μM Pd phosphor, and 0.5% fat-free bovine serum albumin (final volume, 1.0 mL). Respiration was monitored with (*solid circles*) and without (*open circles*) the addition of 100 μM glucose at $t = 0$. After 38 min, the rate of O_2 consumption in the presence of glucose was three times the rate in the absence of glucose. Other additions included 10 mM NaCN, 7 units glucose oxidase, and 50 μg catalase. NaCN stopped O_2 consumption, showing the O_2 was consumed in the mitochondrial respiratory train. Catalase catalyzed the decomposition of H_2O_2, formed in the earlier oxidation of glucose, releasing O_2.

125 μM to 64 μM), 2-1/2 times as large; NaCN was added at 114 min. The decline in [O_2] in the absence of glucose was due to fatty acids in the albumin preparation used here, which can also drive respiration. (Other experiments showed that, with no albumin, the drop in [O_2] is much smaller.) For both conditions, O_2 consumption was completely inhibited by NaCN, confirming the oxidation occurred in the respiratory chain. Oxygen concentration actually increases slightly in both conditions, possibly due to air introduced with the cyanide injections.

In the suspension without glucose, neither injection of glucose oxidase nor later addition of catalase had any measurable effect on [O_2]. For the glucose-containing suspension, the addition of glucose oxidase (at $t = 186$ min) led to a decrease, rapid at first, in [O_2], which dropped from 73 μM to 36 μM in 12 min and from 36 μM to 21 μM in 40 min. The leveling-off of [O_2] at 21 μM is probably due to total depletion of glucose. Thus, starting with 100 μM glucose (and residual fatty acids), the total O_2 consumption was 113 μM, i.e., (125–64) + (73–21) μM. The O_2 consumed in the oxidation of fatty acids was 0.32 μM/min (from the data for cells without glucose) $\times$ (114 $-$ 38) min, or 24 μM. Therefore, the O_2 consumed in glucose oxidation, extracellular and intracellular, was 89 μM. Because 100 μM glucose was consumed, it seems that intracellular glucose oxidation follows the same stoichiometry as extracellular glucose oxidation. The following calculations confirm this.

By fitting [O_2] for $182 \le t \le 234$ min to the form $\alpha + \beta e^{-C(t-182)}$, we find the rate of extracellular O_2 consumption at 182 min to be $(\beta \times C) = 8.89$ μM/min. The specific rate ν is obtained by dividing by the enzyme concentration, 0.125 μM, so $\nu = 71.1\ \text{min}^{-1} = 1.18\ \text{s}^{-1}$. According to Eq. 9, with $B = 0.032$ s and $A = 55.4$ μM s from the experiments of Fig.4 *B* in cell-free PBS, we obtain the glucose concentration at 182 min as 67.9 μM, so that 100 $-$ 67.9 = 32.1 μM glucose was used to drive cellular respiration for $t < 114$ min. From the rate of O_2 consumption with glucose present from $t = 38$ to $t = 114$ min (0.79 μM O_2/min) we subtract the rate of O_2 consumption without glucose (0.32 μM O_2/min) and multiply by the elapsed time (76 min) to obtain the O_2 consumption associated with glucose oxidation during this period, 36 μM. This is 1.1 times the glucose consumption. Although the uncertainties in this calculation are large, it seems clear that the ratio of uptake of glucose by these cancer cells and the associated O_2 consumption is close to 1:1.

The later addition of catalase at 236 min led to an increase in [O_2] from 21 to 40 μM, due to enzyme-catalyzed decomposition of the H_2O_2 formed in the earlier glucose oxidation. The concentration of newly generated O_2 (19 μM) is less than expected from the H_2O_2 produced by glucose oxidation, which would be 1/2(73 $-$ 21) = 26 μM. This difference could result from the fact that H_2O_2, being a strong oxidant, can react with many of biological molecules.

DISCUSSION

Oxygen concentration in biological solutions can be measured rapidly and repeatedly via the decay rate of phosphorescence from a Pd phosphor in solution (Fig. 1). We used this method to study the glucose oxidase-catalyzed reaction of glucose with O_2, which produces gluconic acid and hydrogen peroxide, and the decomposition of hydrogen peroxide into water and oxygen in the presence of catalase. Previous studies of these reactions (18,19) have monitored [glucose] or [H_2O_2], rather than [O_2]; others have used luminescent probes for their studies in similar systems (20–22).

The decay rate $1/\tau$ should be a linear function of [O_2]. To calibrate the instrument, and to confirm the stoichiometry of the glucose oxidation reaction, we measured $1/\tau$ in a series of solutions of glucose in air-saturated PBS with glucose oxidase present. Measured $1/\tau$ was plotted versus [glucose] (Fig. 2 *B*). For [glucose] >250 μM, $1/\tau$ was constant at ~5000 s^{-1}, corresponding to [O_2] = ~0, i.e., complete consumption of O_2. For [glucose] <250 μM, $1/\tau$ decreased linearly with [glucose]. Because [O_2] in air-saturated PBS at 25°C is 267 μM, ~267 μM O_2 reacted completely with ~250 μM glucose, which confirms the 1:1 stoichiometry. From the linear fit of $1/\tau$ versus [glucose], the instrument calibration is established as $1/\tau = 134.5[O_2] + 5002$, where τ is in μs and [O_2] in μM.

The glucose oxidase-catalyzed oxidation of glucose involves four steps, and hence four rate constants and three intermediates (Eqs. 2 and 3). At steady state, the rates of all steps are equal. Plots of [O_2] versus t for [glucose] = 50–300 μM are shown in Fig. 4 *A*. Only β-D-glucose reacts with this catalyst, and the conversion of α to β isomer is slow and can be neglected, except for long times when [glucose] = 50 μM. The initial concentration of the β isomer is ~70% of the total glucose. According to Eq. 4, the reciprocal of the steady-state rate should be a linear function of 1/[glucose]; this is verified in Fig. 4 *B*. Using 1.46 (15) for the mutarotation constant for glucose, we find the rate constant for the reaction of the catalyst E_{ox} with glucose, to form the first intermediate $E_{red}P_1$, to be $k_1 = 3.0 \times 10^4\ \text{M}^{-1}\ \text{s}^{-1}$.

When initial [glucose] is much larger than initial [oxygen], the equation for $d[O_2]/dt$ can be solved explicitly (Eq. 10). Experimental results of [O_2] versus t are fitted to this solution in Fig. 4 *C*. From the fits, we find $k_1 = 2.3 \times 10^4\ \text{M}^{-1}\ \text{s}^{-1}$, between the value given by Gibson et al. (10), $1.6 \times 10^4\ \text{M}^{-1}\ \text{s}^{-1}$, and the value above, $3.0 \times 10^4\ \text{M}^{-1}\ \text{s}^{-1}$. We can also calculate $k_3 = 4.4 \times 10^5\ \text{M}^{-1}\ \text{s}^{-1}$, significantly smaller than the literature value of $2.4 \times 10^6\ \text{M}^{-1}\ \text{s}^{-1}$ (10). Le Barc'H et al. (15) used luminescence intensity to monitor [O_2] during the glucose oxidase-catalyzed oxidation of glucose. They reported a Michaelis constant K_m of 38 $\pm$ 6 mM, as well as some rate data. Direct comparison of our measured rates with those of Le Barc'H et al. (15) is not possible because our measurements were carried out using a different enzyme, a lower enzyme concentration (0.02 vs. 0.8 mg/mL protein),

and a higher temperature (37°C vs. 25°C). If Michaelis-Menten kinetics were followed, V_0 would be proportional to [glucose] for small [glucose] and level off for large [glucose]. Because [glucose] was so low in our measurements, our results (see above) show initial rate proportional to [glucose] with no sign of leveling off, and there is no possibility of measuring K_m. The initial rate V_o is just k_1 times the glucose concentration.

We next studied the catalase-catalyzed H_2O_2 decomposition. The initial rate of reaction was determined from plots of $[O_2]$ versus time obtained from solutions with various $[H_2O_2]$. Then ln(rate) was plotted versus ln($[H_2O_2]$) and fitted to a line. The slope, which should be the reaction order with respect to H_2O_2, changed with temperature. At 37°C, it was 1.27 ± 0.14, consistent with the reaction rate $d[O_2]/dt$ being 1st order in $[H_2O_2]$, as in Eq. 7. However, the slope was 1.69 ± 0.14 for 25°C, suggesting that the reaction is $\frac{3}{2}$-order at the lower temperature. Assuming 1st order kinetics, the rate constant for the decomposition of H_2O_2 at 37°C is 0.177 s^{-1}; writing $d[O_2]/dt$ as $k^*[H_2O_2]^{3/2}$ and seeking the best value of k^* leads to $k^* = 4.49\ M^{-1/2}\ s^{-1}$ at 25°C. We believe that the apparently higher reaction order at 25°C is due to increased importance of the dissociation of the H_2O_2-catalase intermediate, as shown in Fig. 8 *A*. We showed that including this reaction leads to an apparent reaction order with respect to H_2O_2 between 1 and 2.

We next studied glucose oxidation at 37°C in cell culture medium containing 10 mM D-glucose, for which $[O_2]$ was measured as 250 ± 12 μM. When glucose oxidase was added, $[O_2]$ dropped rapidly ($k_c = 0.0846\ s^{-1}$) to zero. To verify that the O_2 was indeed reduced to H_2O_2 as implied by Eqs. 1 and 3, catalase was added to catalyze the decomposition of H_2O_2; $[O_2]$ rose to 86 μM and then, because of the oxidation of remaining glucose, declined to zero. As shown in Fig. 6 *B*, the variation of $[O_2]$ with t was completely explained by assuming that 250 μM H_2O_2 was present (equal to the original $[O_2]$), that the oxidation of glucose occurred with rate constant $k_c = 0.116\ s^{-1}$, and that the reaction $H_2O_2 \rightarrow H_2O + 1/2\ O_2$ occurred with rate constant $k_p = 0.090\ s^{-1}$. This is indicated in Fig. 8 *B*.

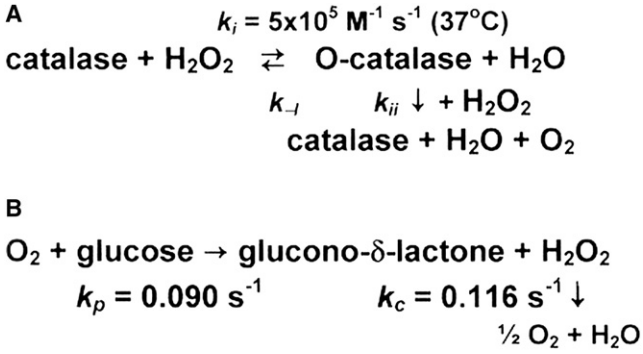

FIGURE 8 Kinetic schemes with rate constants. (*A*) The catalase-catalyzed decomposition of H_2O_2 involves two steps. If $k_{ii}[H_2O_2] >> k_{-i}$ the overall rate is proportional to $[H_2O_2]$, as observed at 37°C. If $k_{ii}[H_2O_2] << k_{-i}$ the overall rate is proportional to $[H_2O_2]^2$. At 25°C, the rate is proportional to $[H_2O_2]^{3/2}$ suggesting that $k_{ii}[H_2O_2]$ is comparable to k_{-i} at 25°C. (*B*) The two enzymatic reactions, one consuming oxygen and producing H_2O_2, and the other producing O_2 from H_2O_2, were combined and the rate constants shown were determined.

Having established that our oxygen measurement method gave valid results in cell culture medium, we studied glucose-driven cellular respiration by starved Jurkat cells (Fig. 7). Two conditions, with and without 100 μM glucose, were used. Glucose-driven respiration began at 38 min; respiration driven by residual fatty acids began somewhat later in the sample without glucose. The rate of consumption of O_2 by cells with glucose was three times the rate by the cells without glucose. For both conditions, addition of cyanide inhibited O_2 consumption completely, showing the oxidations occurred in the mitochondrial respiratory chain. The addition of glucose oxidase 1 h after cyanide had stopped respiration had no effect on $[O_2]$ in the glucose-free condition, but produced a sharp decrease in $[O_2]$ in the glucose-present condition. Subsequent addition of catalase had no effect in the former case, and increased $[O_2]$ in the latter. Both the decrease in $[O_2]$ on glucose oxidase addition and the increase in $[O_2]$ with catalase addition resulted from extracellular glucose oxidation, producing H_2O_2, which was, in turn, decomposed to O_2. Quantitative analysis of this experiment showed glucose/oxygen stoichiometry for cellular oxidation was close to the 1:1 ratio characteristic of extracellular oxidation. The rate of the latter was consistent with our previous measurements.

The results of our experiments show that, by monitoring oxygen concentration via phosphorescence lifetime, one can gain information about the kinetics and mechanism of biochemical reactions. For the glucose oxidase-catalyzed oxidation of glucose, we confirmed the stoichiometry and found precise values of several rate constants. (These measurements also established the calibration of our instrument.) For the catalase-catalyzed decomposition of hydrogen peroxide, we showed that, although the simple mechanism (Eqs. 4 and 5) explained the reaction order at 37°C, it failed to do so at 25°C. We suggested that, at 25°C, the reverse reaction to Eq. 4 is important; including it can explain the observed reaction order of 1.67. (Because the reaction order at 37°C, 1.27 ± 0.14, may be significantly greater than unity, this reaction may also be important at 37°C, but less so.) The oxygen-measurement technique also showed its utility in more complicated systems, in which both glucose oxidation and hydrogen peroxide decomposition occurred, or in which there was intracellular as well as extracellular oxidation of glucose. In particular, we showed that the glucose-oxygen ratio for intracellular oxidation was essentially the same as for extracellular (glucose oxidase-catalyzed) oxidation.

REFERENCES

1. Vanderkooi, J. M., G. Maniara, T. J. Green, and D. F. Wilson. 1987. An optical method for measurement of dioxygen concentration based upon quenching of phosphorescence. *J. Biol. Chem.* 262:5476–5482.

2. Rumsey, W. L., J. M. Vanderkooi, and D. F. Wilson. 1988. Imaging of phosphorescence: a novel method for measuring the distribution of oxygen in perfused tissue. *Science.* 241:1649–1651.

3. Pawlowski, M., and D. F. Wilson. 1992. Monitoring of the oxygen pressure in the blood of live animals using the oxygen dependent quenching of phosphorescence. *Adv. Exp. Med. Biol.* 316:179–185.

4. Lo, L. W., C. J. Koch, and D. F. Wilson. 1996. Calibration of oxygen dependent quenching of the phosphorescence of Pd-meso-tetra (4-carboxyphenyl) porphine: a phosphor with general application for measuring oxygen concentration in biological systems. *Anal. Biochem.* 236:153–160.

5. Tao, Z., H. G. Withers, H. S. Penefsky, J. Goodisman, and A. -K. Souid. 2006. Inhibition of cellular respiration by doxorubicin. *Chem. Res. Toxicol.* 19:1051–1058.

6. Tao, Z., S. S. Ahmad, H. S. Penefsky, J. Goodisman, and A. -K. Souid. 2006. Dactinomycin impairs cellular respiration and reduces accompanying ATP formation. *Mol. Pharm.* 3:762–772.

7. Tao, Z., H. S. Penefsky, J. Goodisman, and A. -K. Souid. 2007. Caspase activation by anticancer drugs: the caspase storm. *Mol. Pharm.* 4:583–595.

8. Tao, Z., M. P. Morrow, H. S. Penefsky, J. Goodisman, and A. -K. Souid. 2007. Study on caspase-induced mitochondrial dysfunction by anticancer drugs. *Curr. Drug Ther.* 2:233–235.

9. Tao, Z., J. Goodisman, and A. -K. Souid. 2008. Oxygen measurement via phosphorescence: reaction of sodium dithionite with dissolved oxygen. *J. Phys. Chem. A.* 112:1511–1518.

10. Gibson, Q. H., B. E. P. Swoboda, and V. Massey. 1964. Kinetics and mechanism of action of glucose oxidase. *J. Biol. Chem.* 239:3927–3934.

11. Swoboda, B. E. P., and V. Massey. 1965. Purification and properties of the glucose oxidase from. *Aspergillus niger. J. Biol. Chem.* 240:2209–2215.

12. Keilin, D., and E. F. Hartree. 1952. Specificity of glucose oxidase (notatin). *Biochem. J.* 50:331–341.

13. Keilin, D., and E. F. Hartree. 1952. Biological catalysis of mutarotation of glucose. *Biochem. J.* 50:341–348.

14. Los, J. M., L. B. Simpson, and K. Wiesner. 1956. The kinetics of mutarotation of D-glucose with consideration of an intermediate free-aldehyde form. *J. Am. Chem. Soc.* 78:1564–1568.

15. Le Barc'H, N., J. M. Grossel, P. Looten, and M. Mathlouthi. 2001. Kinetic study of the mutarotation of D-glucose in concentrated aqueous solution by gas-liquid chromatography. *Food Chem.* 74: 119–124.

16. Sies, H., and B. Chance. 1970. The steady state level of catalase compound I in isolated hemoglobin-free perfused rat liver. *FEBS Lett.* 11:172–176.

17. Deisseroth, A., and A. L. Dounce. 1970. Catalase: physical and chemical properties, mechanism of catalysis, and physiological role. *Physiol. Rev.* 50:319–375.

18. Beers, Jr., R. F., and I. W. Sizer. 1952. A spectrophotometric method for measuring the breakdown of hydrogen peroxide by catalase. *J. Biol. Chem.* 195:133–140.

19. Bateman, Jr., R. C., and J. A. Evans. 1995. Using the glucose oxidase/peroxidase system in enzyme kinetics. *J. Chem. Educ.* 72:A240–A241.

20. Bare, W. D., C. V. Pham, M. Cuber, and J. N. Demas. 2007. An improved method for studying the enzyme-catalyzed oxidation of glucose using luminescent probes. *J. Chem. Educ.* 84:1511–1514.

21. Carraway, E. R., J. N. Demas, B. A. DeGraff, and J. R. Bacon. 1991. Photophysics and photochemistry of oxygen sensors based on luminescent transition-metal complexes. *Anal. Chem.* 53:337–342.

22. Demas, J. N., B. A. DeGraff, and P. B. Coleman. 1999. Oxygen sensors based on luminescence quenching. *Anal. Chem.* 71:793A–800A.